Environmental Effects on Subcritical Delamination of Dielectric and Metal Films from Organosilicate Glass (OSG) Thin Films

Y. Lin, J.J. Vlassak, T.Y. Tsui[1], and A.J. McKerrow[1]
DEAS, Harvard University, 29 Oxford Street, Cambridge, MA 02138, USA
[1]Silicon Technology Development, Texas Instruments Inc., Dallas, TX 75243, USA

ABSTRACT

Subcritical delamination of dielectric and metal films from organosilicate glass (OSG) thin films was studied in controlled ambient with different levels of relative humidity and in aqueous environments of varying pH. The material systems studied include OSG/SiO_2, OSG/TaN and OSG/SiN_x. For both sets of experiments, subcritical crack growth in OSG is found to be described by a model originally developed for soda-lime silicate glass. The threshold energy release rate for water molecule-assisted cracking varies linearly with the natural logarithm of water partial pressure. In aqueous environments, the threshold value decreases linearly with increasing pH in accordance with a simple model. The slope of crack growth rate curve also decreases with increasing pH.

INTRODUCTION

Organosilicate glasses (OSG) are leading candidates among new low-k dielectric materials that are being assessed for use as interlayer dielectric (ILD) in high-performance interconnects. OSG is essentially silicon dioxide in which a fraction of the Si-O bonds have been replaced with bonds to organic groups, typically methyl groups (e.g., $-CH_3$). As a result, OSG has a network structure similar to that of fused silica, but less dense because of the presence of the $-CH_3$ groups. The dielectric constant is reduced from 4 to approximately 2.8 – 3.1. A consequence of this change in bonding and density is that the mechanical properties (hardness, toughness, modulus, etc.) of OSG films are inferior to those of silica. During the many wet-processing steps involved in semiconductor device fabrication, OSG films are subject to mechanical loads in aggressive chemical environments. Typical examples include loads that arise during chemical-mechanical polishing (CMP) or dicing, as well as loads due to residual stresses in the film stack. Under such conditions there is a concern that OSG films may be vulnerable to stress-corrosion, leading to delamination of the film stack. To better understand this issue, we present an investigation of subcritical delamination of various dielectric and metal barrier films from OSG thin films in controlled ambient with different levels of relative humidity and in aqueous environments of varying pH.

EXPERIMENTAL DETAILS

Subcritical crack growth was studied by means of the four-point bending technique. To this purpose, 500 nm OSG films were deposited onto 200 mm silicon wafers using PECVD. The OSG films were capped with three different barrier layers: 80 nm of SiN_x, 30 nm of TaN, and 250 nm of PECVD SiO_2 (TEOS precursor). The TaN wafers were subsequently sputter coated with 150 nm of Cu; the SiN_x and SiO_2 wafers were coated with a 70 nm adhesion layer of Ti, followed by 300 nm of Cu. Four-point-bend samples were prepared by bonding these wafers to SiN_x-coated silicon wafers using a spin-coated epoxy. The epoxy was cured at 90°C for 60 minutes under a pressure of 8 kPa. After bonding, the sandwiched structures were diced into 60

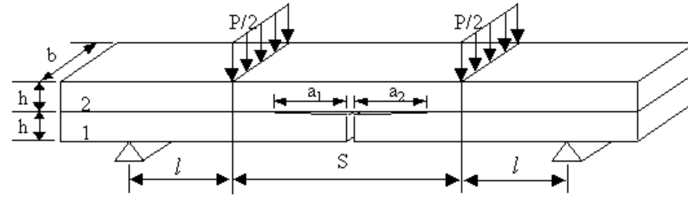

Figure 1. A sandwiched, notched four-point bend specimen

mm x 6 mm specimens. Finally, a notch was machined to within approximately 60 μm of the interface using a high-speed dicing saw.

Figure 1 is a schematic representation of the specimen configuration in the four-point bend test. As the specimen is loaded in pure bending, a crack emanates from the notch and propagates along the weakest interface in the film stack. The energy release rate G at the crack tip can be expressed as [1, 2]

$$G = \frac{21P^2 l^2 (1-\nu^2)}{16Eb^2 h^3}, \tag{1}$$

where E and ν are the elastic modulus and Poisson's ratio of the Si substrate, P is the load, l the distance between the inner and outer loading pins, b the width of the specimen, and h the wafer thickness. During crack propagation, the compliance of the beam is a function of the crack length. Hence, the averaged crack growth rate v can be evaluated from the rate of change of the sample compliance and is given by the following equation [3]

$$v = \frac{1}{2}\cdot\frac{d(a_1 + a_2)}{dt} = \frac{4Ebh^3}{21(1-\nu^2)l^2}\frac{d}{dt}\left(\frac{H}{P}\right), \tag{2}$$

where H is the deflection of the beam.

Tests were conducted using a high-stiffness, low-drift four-point bend tester with in-situ environmental cell. The environmental cell provides control over the relative humidity during the test and also makes it possible to run experiments in aqueous environment. In this study, buffer solutions were prepared from HCl, KCl, and KOH solutions. Titration was conducted to achieve the desired pH values. The pH values were measured using a FUTURA™ electrode from BECKMAN. Before each measurement, the electrode was calibrated with standard pH buffer solutions provided by VWR.

A two-step method was used for the experiments. First, the sample was preloaded in a shortened-S configuration, where S is the span between the two inner loading pins (S = 12 mm), until delamination occurred. The plateau load at which the crack propagates along the interface was used to determine the critical energy release rate for delamination. Next, the sample was unloaded and the spacing between the inner loading pins increased to 36 mm. After reloading the sample to a predetermined value, the displacement was held constant and load relaxation was recorded as the crack continued to grow. Equations (1) and (2) were then used to derive crack velocity as a function of applied crack extension force. Throughout all loading steps, the displacement rate was held constant at 0.5 μm/s. All experiments were conducted at 26°C and the total temperature drift was less than 1°C over a period of 24 hours. To minimize the effect of vibrations on the velocity measurements, the entire test assembly was placed on a vibration isolation table.

The crack path was identified by means of X-ray photoelectron spectroscopy (XPS). A Surface Science XPS system, model SSX-100, and Al K_{α} radiation was used for all measurements. The characteristic depth is approximately 20 Å. XPS was combined with a 4 keV Ar^+ ion beam at an incident angle of 45° to obtain depth profiles.

RESULTS AND DISCUSSION

Figure 2 (a) shows typical XPS spectra for a TaN/OSG sample. One of the fracture surfaces consists of OSG, but the character of the other surface is less clear. After 60 s of Ar^+ sputtering, however, peaks for Ta and N become evident. Delamination therefore occurs within the OSG layer, parallel to the TaN/OSG interface. The thickness of the OSG remaining on the TaN side was estimated to be approximately 70 Å. Figure 2 (b) depicts XPS spectra for a SiN_x/OSG sample. The N peak for one of the fracture surfaces indicates that this surface consists of SiN_x, while the other spectrum is characteristic for OSG. It can therefore be concluded that the crack propagates along SiN_x/OSG interface. The interpretation of the XPS spectra for the SiO_2/OSG samples shown in Fig. 2 (c) is not as straightforward. Analyses of both fracture surfaces result in very similar spectra, even after 60 second of Ar^+ sputtering. Since TEOS-based SiO_2 also contains a certain amount of carbon, it was necessary to perform XPS on blanket films of SiO_2 and OSG in order to identify the crack path. A comparison of the composition of the fracture surfaces before and after Ar^+ sputtering (see Table 1) indicates that one surface consists of OSG, while the other of TEOS-based SiO_2. Hence, delamination takes place at the SiO_2/OSG interface.

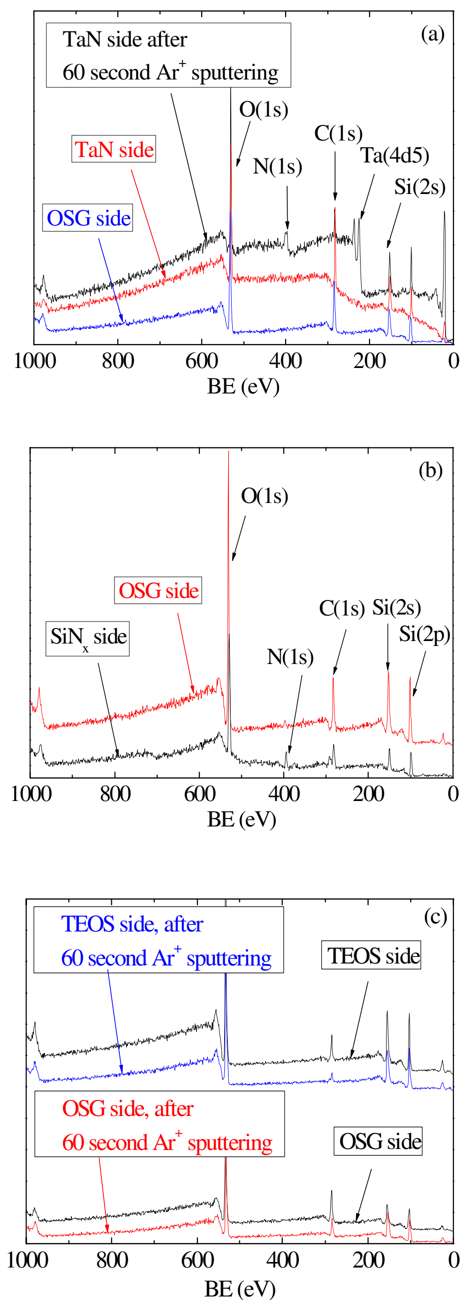

Figure 2. XPS spectra of fracture surfaces, (a) TaN/OSG, (b) SiNx/OSG, (c) SiO_2/OSG.

Figure 3 shows subcritical crack growth data for the three material systems in ambients with controlled relative humidity. The curves in Figure 3 are all similar indicating that sub-critical fracture in these systems is controlled by the same mechanism. With increasing relative humidity, the stress-corrosion thresholds shift to lower values of *G*. Stress-corrosion cracking assisted by water molecules has been modeled in bulk glass [4, 5] and extended to thin films [6], where a sinh law was used to fit the reaction-dominated regime at low driving force. This model provides a good

Table 1. Composition of fracture surfaces of a SiO_2/OSG sample and blanket SiO_2 and OSG films. Sputter conditions are: 4 keV Ar^+ for 60 s.

Surfaces	O (at.%)	C (at.%)	Si (at.%)
SiO_2 side	53	16	31
SiO_2 side (after sputtering)	54	10	36
Blanket SiO_2	54	15	31
Blanket SiO_2 (after sputtering)	55	9	36
OSG side	43	31	26
OSG side (after sputtering)	44	19	37
Blanket OSG	47	29	24
Blanket OSG (after sputtering)	42	20	38

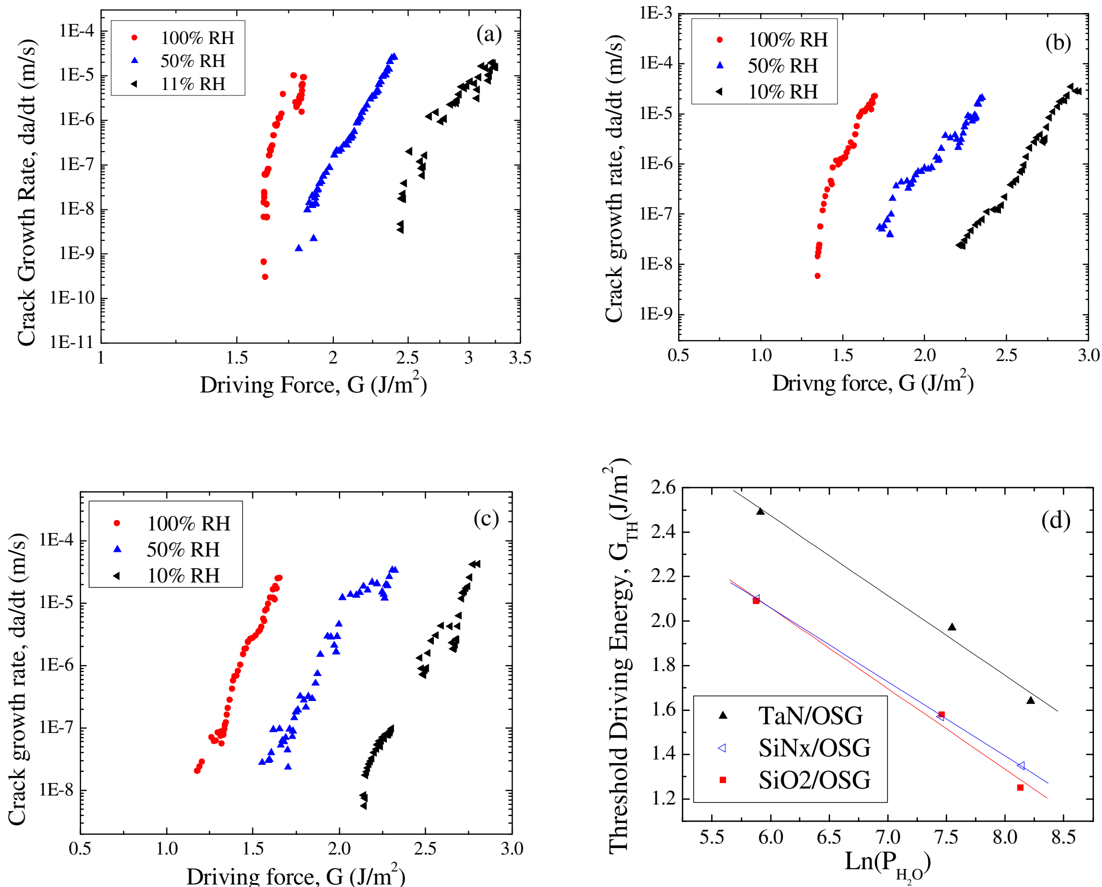

Figure 3. (a) Dependence of crack velocity on applied driving force for TaN/OSG, (b) SiN_x/OSG, (c) SiO_2/OSG, (d) Dependence of threshold value on water partial pressure.

description of the data presented in Fig. 3 and results in a bond density of 1.2×10^{19} m^{-2}, which is comparable to the number reported by Wiederhorn [4] for bulk glass. Figure 3(d) shows that the threshold energy release rate below which there is no crack growth varies linearly with the natural logarithm of water partial pressure in agreement with previous reports [4-6].

In aqueous conditions, the solubility of silica increases with increasing pH values due to the following reactions [7]:

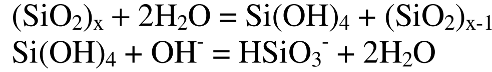

$$(SiO_2)_x + 2H_2O = Si(OH)_4 + (SiO_2)_{x-1}$$
$$Si(OH)_4 + OH^- = HSiO_3^- + 2H_2O$$

The transportation flux of OH^- ions from the bulk of the solution to the crack tip is given by

$$F_t = -D_{OH}\frac{\partial C}{\partial x} = \frac{D_{OH}}{\delta}\left(10^{-pOH} - \left[OH^-\right]_0\right), \qquad (3)$$

Where D_{OH} is the diffusion coefficient of the OH^- ions, δ is the thickness of the diffusion layer, and $[OH^-]_0$ is the OH^- concentration at the crack tip. The reaction flux at the crack tip can be written as [5]

$$F_r = k_0\left(\left[OH^-\right]_0\right)^n \sinh\left(\frac{G-2\gamma}{2NkT}\right), \qquad (4)$$

Where k_0 is the reaction constant, n is the order of reaction, and 2γ is related to the change in chemical potential μ as a result of the reaction

$$2\gamma = N\left(\Delta\mu^* - nkT\ln\left(10^{-pOH}\right)\right) = N\left(\Delta\mu^* + nkT\ln 10\cdot pOH\right), \qquad (5)$$

Where N is the number of bonds per unit area. If r is the bond length and N_{av} is Avogadro's Number, the crack velocity can be written as

$$v = \frac{da}{dt} = \frac{r^3 N_{av} F_r}{n}, \qquad (6)$$

Equating F_t and F_r makes it possible to eliminate $[OH^-]_0$ from Equation (4). Assuming first order kinetics and combining Equations (3), (4) and (6) yields the expression for the crack growth rate

$$v = \frac{r^3 N_{av} k_0 10^{-pOH}}{1 + \frac{k_0\delta}{D_{OH}}\sinh\left(\frac{G-2\gamma}{2NkT}\right)}\sinh\left(\frac{G-2\gamma}{2NkT}\right), \qquad (7)$$

Figure 4 shows subcritical crack growth curves for the SiO_2/OSG system in various pH buffer solutions and compares them to data taken in environments with different levels of relative humidity. The crack velocity obtained in acidic solutions is the same as the velocity at 100% RH. An increase in pH of the solution results in a significant increase in crack velocity as indicated in Equation (7). Figure 5 (a) shows that the threshold energy release rate decreases linearly with increasing pH (or decreasing pOH) in agreement with Equation (5). The slope of the crack growth curves decreases with increasing pH as illustrated in Fig 5 (b). This was also observed by Wiederhorn and Johnson [8] for a number of bulk glasses and may be attributed to a pH-dependence of the activation volume of the chemical reaction controlling fracture.

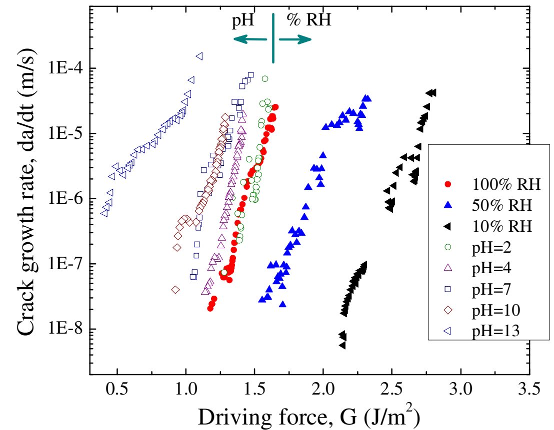

Figure 4. Comparison of crack growth rate curves for SiO_2/OSG in moisture and in pH buffers.

CONCLUSIONS

The effect of water partial pressure and

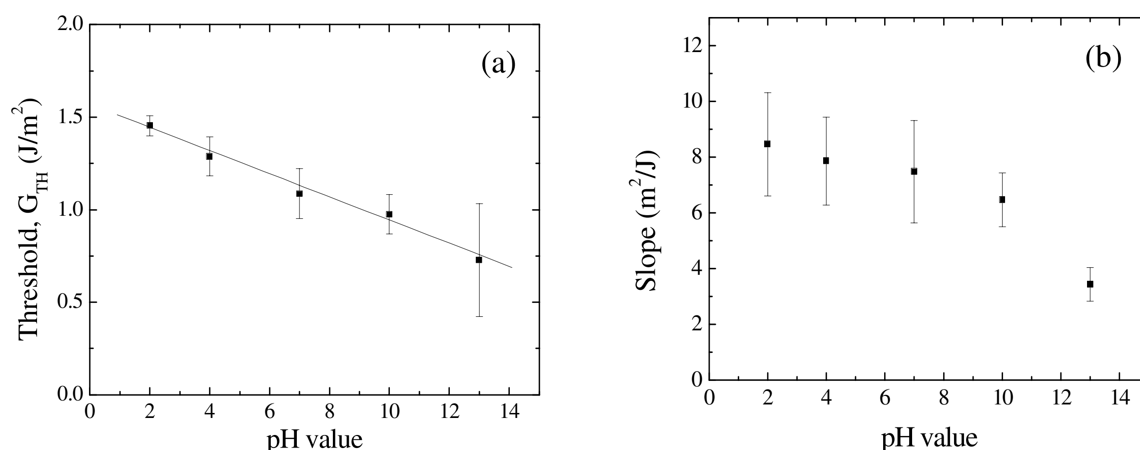

Figure 5. Dependence of threshold energy release rate (a) and slope (b) on pH values.

pH on subcritical delamination of a number of barrier films from OSG coatings has been investigated. For both SiN_x and SiO_2 films, the delamination takes place at the OSG/barrier film interface, while the crack in the TaN system propagates within the OSG film. Despite the presence of organic groups in the OSG film, the behavior of these film stacks is remarkably similar to that of bulk silicate glass. The threshold value for crack growth decreases linearly with the logarithm of the water partial pressure and with pH, while the slope of the crack velocity curves in aqueous environment decreases with increasing pH.

ACKNOWLEDGMENTS

The authors wish to thank Professor G. Golovchenko for use of the dicing saw. Financial support from the Division of Engineering and Applied Sciences, from the Harvard MRSEC (DMR-98-09363), and from the National Science Foundation (DMR-0133559; DMR-0215902) is gratefully acknowledged.

REFERENCES

1. P. G. Charalambides, J. Lund, A. G. Evans and R. M. McMeeking, *Journal of Applied Mechanics,* **56**, 77 (1989).
2. Q. Ma, H. Fujimoto, P. Flinn, V. Jain, F. Adibi-Rizi, F. Moghadam and R. H. Dauskardt, in *Materials Reliability in Microelectronics V,* edited by A. S. Oates, W. F. Filter, R. Rosenberg, A. L. Greer and K. Gadepally (Mater. Res. Soc. Symp. Proc. **391**, Pittsburgh, PA, 1995), pp. 91-96.
3. Q. Ma, *Journal of Materials Research,* **12** (3), 840 (1997).
4. S. M. Wiederhorn, *Journal of The American Ceramic Society,* **50** (8), 407 (1967).
5. R. E. Cook and E. G. Liniger, *Journal of The American Ceramic Society,* **76** (5), 1096 (1993).
6. M. Lane, R. Dauskardt, Q. Ma, H. Fujimoto and N. Krishna, *Materials Research Society Symposium Proceedings,* **563,** 251 (1999).
7. R. K. Iler, *The Chemistry of Silica: Solubility, Polymerization, Colloid and Surface Properties and Biochemistry of Silica,* (John Wiley & Sons, 1979) p. 47.
8. S. M. Wiederhorn and H. Johnson, *Journal of The American Ceramic Society,* **56** (4), 192 (1973).